NUMERICAL STUDY OF UNSTEADY FLOW AND EXCITING FORCE FOR SWEPT TURBOMACHINERY BLADES

by

Di ZHANG*[*]*, Jiao-Bin MA, and Qi JING

MOE Key Laboratory of Thermo-Fluid Science and Engineering,
School of Energy and Power Engineering, Xi'an Jiaotong University, Xi'an, China

Original scientific paper
DOI: 10.2298/TSCI160205199Z

The aerodynamic performance of blade affects the vibration characteristics and stable operation of turbomachinery closely. The aerodynamic performance of turbine stage can be improved by using swept blade. In this paper, the Reynolds-averaged Navier-Stokes method and the renormalized group k-ε turbulence mode were adopted to investigate the unsteady flow characteristics and excitation force of swept blade stage. According to the results, for the swept blade, the fluid of boundary layer shifts in radial direction due to the influence of geometric construction. It is observed that there is similar wake development for several kinds of stators, and the wake has a notable effect on the boundary layer of the rotor blades. When compared with straight blade, pressure fluctuation of forward-swept blade is decreased while the pressure fluctuation of backward-swept blade is increased. The axial and tangential fundamental frequency excitation force factors of 15° forward-swept blade are 0.139 and 0.052, respectively, which are the least, and all excitation force factors are in the normal range. The excitation factor of the forward-swept blade is decreased compared with straight blade, and the decreasing percentage is closely related to the swept angle. As for backward-swept blades, the situation is the other way around. Additionally, the change of axial excitation factor is more obvious. So the vibration reduction performance of forward-swept blade is better.

Key words: *swept blade, unsteady flow, exciting force, numerical investigation*

Introduction

The aerodynamic characteristics and flow in the turbomachine are highly unsteady. It is of great significance to investigate the unsteady flow and the unsteady aerodynamic force for the design and optimization of turbomachine. With the development of computational fluid dynamics, numerical simulation method has been widely used to study the unsteady flow in turbines. Chaluvadi *et al.* [1] numerically studied the aerodynamic characteristics of the turbine high-pressure cylinder, and the results show that the main cause of the unsteady characteristics of the downstream rotor are the blade wakes interference and secondary flow interference. The numerical results of reference [1] were analyzed by Lampart *et al.* [2]. The development of secondary flow, separation flow and wakes was shown clearly with figures, and the gas leak behaviors at tip and root of blades were analyzed. The flow loss coefficients in the blades of high-pressure cylinder are revealed through research. In the research by Carolus and Beiler. [3], the Reynolds-averaged Navier-Stokes (RANS) method was adopted to research the influence

* Corresponding author; e-mail: zhang_di@mail.xjtu.edu.cn

of wakes to the fluid in rotor. It is obtained that the secondary flow shifted to the mid-span position of rotor blade, and the pressure presented coupled between wakes and main flow.

Recently much attention has been paid to the development of swept blade for the improvement of aerodynamic performance. The traditional design and optimization of axial flow turbine blades incorporates radial stacking (RS), *i. e.* the centers of gravity of the individual blade sections are stacked on a radial line. A blade has a forward/backward sweep (FSW/BSW) if the sections of a RS datum blade are shifted parallel to their chord in such a way that a blade section under consideration is upstream/downstream of the neighboring blade section at lower radius [4]. As a valuable supplement to blade optimization achievable with RS techniques, a comprehensive summary is given in [5] and [6] about non-radial stacking (NRS). It is obtained that NRS offers an increased capability for the reduction on near-end wall and tip clearance losses as well as the control of secondary flows and radial migration of high-loss fluid. In 1990s, Wennerstrom [7] carried out an experimental study of FSW blade in supersonic compressor, and the results presented that FSW design kept a better aerodynamic quality with a faster velocity. A numerical study was conducted to research the effect of sweep blade on the performance of wells turbine by Kim *et al.* [8]. It is shown that the numerical method can predict the effect of sweep blade quite well.

Of all the previous studies, much attention has been paid to the pressure distribution and the boundary layer of the blade. Little research has been done on the unsteady flow and aerodynamic force caused by the swept blade. The swept blade has notable effects on the unsteady flow and excitation force because of the variation of clearance between rotor and stator. In this paper, the RANS method and the renormalized group (RNG) k-ε turbulence mode were adopted to analyze the unsteady flow characteristics and excitation force of swept blade and straight blade stages. The pressure distribution, stage efficiency and the excitation force factor for different kinds of blades were obtained and compared with each other, thus providing the reference data for the vibration reduction by using swept blade.

Numerical method

Physical model

The stacking line is a connecting line through center of gravity for every blade sections from root to tip. It is pointed by Sasaki and Breugelmans [9] that it's the stacking line of swept blade shifts parallel to upstream/downstream in axial direction. The design parameter of swept blade usually includes swept angle and swept height. In order to simplify the blade construction, quadratic curve is adopted to fit the stacking line, and a sweep angle α is defined to replace the swept angle ϕ, and swept height h. In this way, the flow loss at the transition position of swept blade from swept to straight is reduced because of the smooth transition position.

Although there is some difference between the swept blade studied in this paper and the traditional swept blade, using one parameter to define the blade has little effect on geometric construction of models, thus the models constructed can also be used to reveal the action mechanism of swept blades. Figure 1 shows the stacking lines of the swept blades and the 3-D models of forward-swept (FSW), back-swept (BSW), and straight blades (STR). Seven kinds of stator swept blades were built with different swept angles that are, respectively –15°, –10°, –5°, 0°, 5°, 10°, and 15°.

In this paper the turbine swept blade stage investigated is composed of an intake passage, a stator, a rotor and an exhaust passage, and the clearance between rotor and stator is equally divided into two parts along the axial direction. The length of the intake passage is

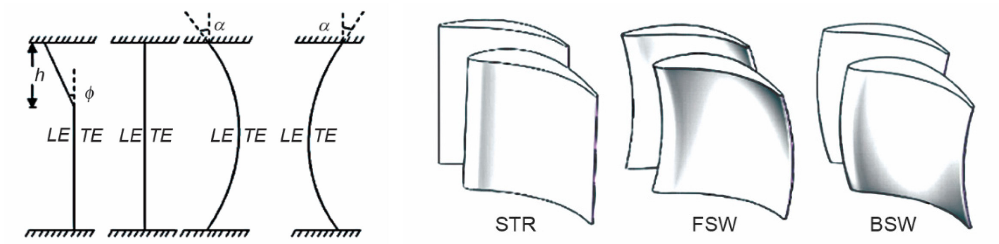

Figure 1. The stacking line of blade and 3-D model of stator blade; LE – the leading edge, which is the forward edge of airfoil or blade, TE – the trailing edge, which is the rear edge of airfoil or blade

three times the axial chord length of the stator blade, and the length of the exhaust passage is five times the axial chord length of rotor blade. Simplified model usually are adopted to save the computing resource. For the stage studied there are 40 stator blades and 65 rotor blades, thus a simplified model with 8 stator blades and 13 rotor blades are used. Figure 2 shows the numerical model and the grid of computation domain for stator and rotor blades. The computation domain with 1.85 million nodes is chosen for the final calculation by a grid-independent validation. The block-structured grid is adopted in order to conform to the requirements of the complex structure and topological relations of the intake passage, cascade passage, and exhaust passage. For calculation the hexahedral grid with an O type mesh near the blade wall and an H type grid in other region are used.

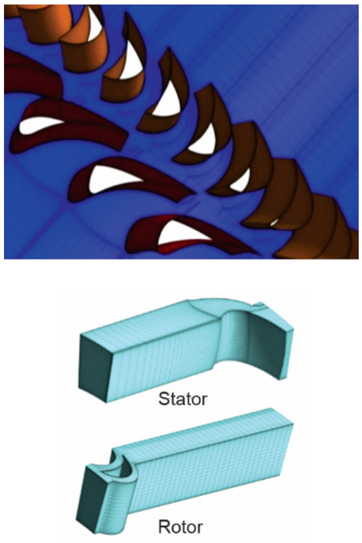

Figure 2. Calculation model and the grid of the stator and rotor *(for color image see journal web-site)*

Computational method and boundary conditions

In the numerical simulations the flow is considered to be 3-D and unsteady. According to the fundamental theory of CFD, the Navier-Stokes equations are solved to obtain the complex flow in the turbine stage. Besides, the widely used RANS method is also applied. The equations governing the fluid dynamics are based on the conservation equations of mass, momentum, and energy. The continuity equation is:

$$\frac{\partial \rho}{\partial t}+\frac{\partial(\rho u)}{\partial x}+\frac{\partial(\rho v)}{\partial y}+\frac{\partial(\rho w)}{\partial z}=0 \tag{1}$$

The momentum equation is:

$$\frac{\partial U}{\partial t}+\frac{\partial(E-E_v)}{\partial x}+\frac{\partial(F-F_v)}{\partial y}+\frac{\partial(G-G_v)}{\partial z}=0 \tag{2}$$

The energy equation is:

$$\frac{\partial(\rho T)}{\partial t}+\mathrm{div}(\rho U T)=\mathrm{div}\left(\frac{\lambda}{C_p}\mathrm{grad}T\right)+S_T \tag{3}$$

where S_T is the viscous dissipation term.

As the turbulence model and ideal gas state equation are adopted to set-up a closed-form equation system, various parameters, including $u, v, w, t, k, \varepsilon$, and T, can be obtained by numerical calculation. The ideal gas state equation is:

$$p = \rho \mathrm{R} T \tag{4}$$

In this paper, the RNG k-ε turbulence model developed by Yakhot and Orszag [10], which expands the unsteady Navier-Stokes equation via GAUSS statistics, is adopted for numerical calculations. The effects of small-scale vortices are eliminated by spectrum analysis. The ε term is added to non-linear addition term expressed as R_ε in RNG k-ε turbulence model, which is different from the standard k-ε equation. Simulation accuracy of the rotational flow is improved by the additional R_ε. The transport equations for RNG k-ε turbulence model are given:

$$\frac{\partial(\rho k)}{\partial t} + \frac{\partial(\rho k u_i)}{\partial x_i} = \frac{\partial}{\partial x_j}\left(\alpha_k \mu_{\mathrm{eff}} \frac{\partial k}{\partial x_j}\right) + G_k + \rho\varepsilon \tag{5}$$

where G_k is generation item for turbulent kinetic energy due to the velocity gradient.

$$\frac{\partial(\rho \varepsilon)}{\partial t} + \frac{\partial(\rho \varepsilon u_i)}{\partial x_i} = \frac{\partial}{\partial x_j}\left(\alpha_\varepsilon \mu_{\mathrm{eff}} \frac{\partial \varepsilon}{\partial x_j}\right) + \frac{C_{1\varepsilon}^*}{k} G_k - C_{2\varepsilon}\rho\frac{\varepsilon^2}{k} - R_\varepsilon \tag{6}$$

$$R_\varepsilon = \frac{C_\mu \rho \eta^3 \dfrac{1-\eta}{\eta_0}}{1+\beta\eta^3}\frac{\varepsilon^2}{k} \tag{7}$$

In this study the ideal air is used as the working fluid. The reference pressure is set as 1 atm, and a total pressure of 40 °C and a total temperature of 20 kPa are used at the inlet. At the outlet the static pressure is set as 0 Pa. The rotational speed of the turbine is 5000 rpm. The transient frozen rotor method is applied to the interface between stators and rotors.

Results and discussion

Flow characteristics

Figures 3 and 4 show the streamline distribution at the pressure surface and suction surface for the 15° FSW, 15° BSW and straight stator blades, respectively. As observed, for the STR the streamline at the mid-span position is quite straight and uniform, but the streamline near the end wall on pressure surface shifts to corner. The streamline near the end wall on suction surface shifts to mid-span, which maybe caused by the passsage vortex. It is worth

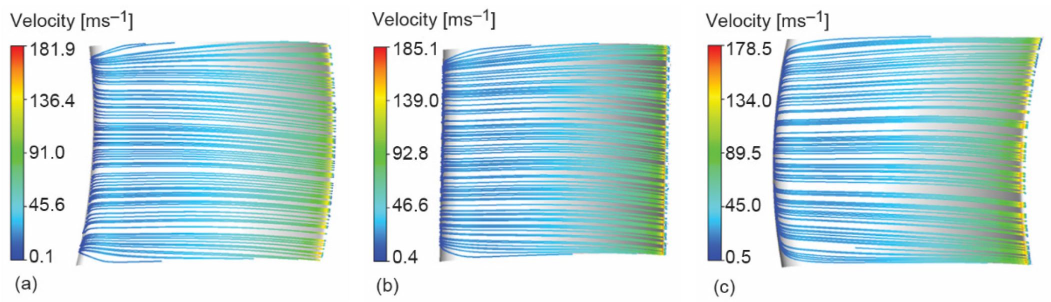

Figure 3. The streamline of stator on pressure surface; (a) 15° FSW, (b) STR, (c) 15° BSW
(for color image see journal web-site)

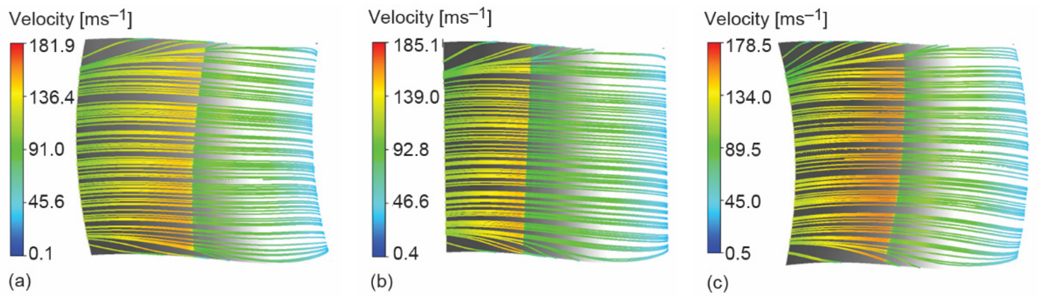

Figure 4. The streamline of stator on suction surface; (a) 15° FSW, (b) STR, (c) 15° BSW
(for color image see journal web-site)

noting that the spanwise migration of the streamline near the end wall has been weakened by the FSW blade, and the situation for the back-swept blade is the other way around.

Figure 5 shows the blade profile at the mid-span position and blade ends for the FSW blade. Compared with the blade profile at the mid-span position, the blade profile at the blade ends shows a more anterior position. As a result, the flow at the blade ends is forced to move to the mid-span position on pressure surface, and the flow with low velocity at the blade ends is reduced. At the trailing edge of the suction surface, the flow is forced to move to the end walls, thus effectively reducing the shifting to the mid-span position. As for the BSW blade, the flow characteristic is the other way around. The FSW blade can effectively control the flow in the span direction of the stator blade by reducing the accumulation of low energy fluid at corner and the effect of span direction migration, thus resulting in a more stable flow condition for the downstream.

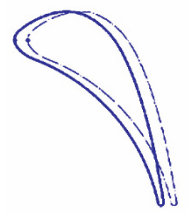

Figure 5. The FSW blade profile at mid-span position (imaginary line) and ends

Wakes and static pressure distribution

Because of the influence of the trailing edge of stator blades, there exists a velocity gradient on pressure surface and suction surface. The mixing of fluid from these two sides forms a wake with high turbulence, which has a notable impact on the downstream cascade flow. The distribution of static entropy in the mid-span position of the STR is shown in fig. 6, and it is similar with the cases with FSW and BSW blades. The wakes have notable effects on the boundary layer of the rotor blades. The wake development on the second half of rotor blades is quicker than the first half, and the wake development on the suction surface is quicker than that on the pressure surface.

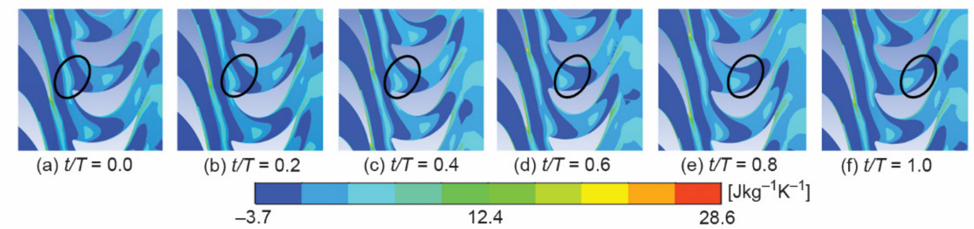

Figure 6. Static entropy contours and the development of stator wakes for STR
(for color image see journal web-site)

The pressure distribution around the blade is one of the most important parameters to measure blade aerodynamic performance, which not only determines the work done by the blade, but also affects the aerodynamic efficiency. Figure 7 shows pressure fluctuations of rotor blade. Because of the influence of upstream wake, the pressure on the rotor blade surface is highly unsteady. The unsteady wake also leads to the unsteady aerodynamic force of rotor blade. Conclusion can be obtained by the unsteady pressure fluctuation during the former 2/3 chord length of rotor blade's suction surface and the latter 4/5 chord length of pressure surface, which shows that the wake of stator blades has much influence on this area. Moreover, compared with STR, the pressure fluctuation of FSW blade is decreased while the pressure fluctuation of BSW blade is increased. This is because the gap between stator and rotor blade of FSW blade is increased, which is beneficial to the wake dissipation and weaken the wake's unsteady impact on the downstream. As to BSW blade, the situation is the other way around.

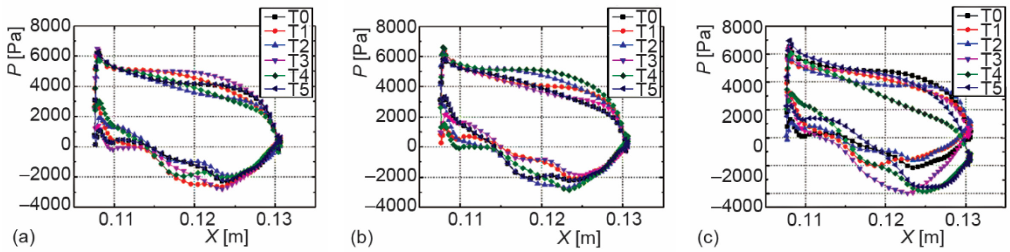

Figure 7. The static pressure distribution of rotor on mid-span; (a) 15° FSW, (b) STR, (c) 15° BSW

Excitation force factor

As for the turbine under the working condition, the periodic excitation force is unavoidable due to the unsteady flow field, and it affects the working performance and service life of the turbine. Figure 8 shows the variation of axial force and tangential force with time for the swept blade and STR. The fast Fourier transform is adopted in this thesis for the spectral analysis. It is found that the tangential and axial aerodynamic force of the FSW blade is significantly decreased compared with straight blade, while the situation for the BSW blade is the other way around. As for the rotor with STR, the tangential and axial frequency spectrum characteristics shows a large amplitude of fundamental frequency excitation force at f =3333.33 Hz, which is in good coincidence with the theoretical value (40×83.33).

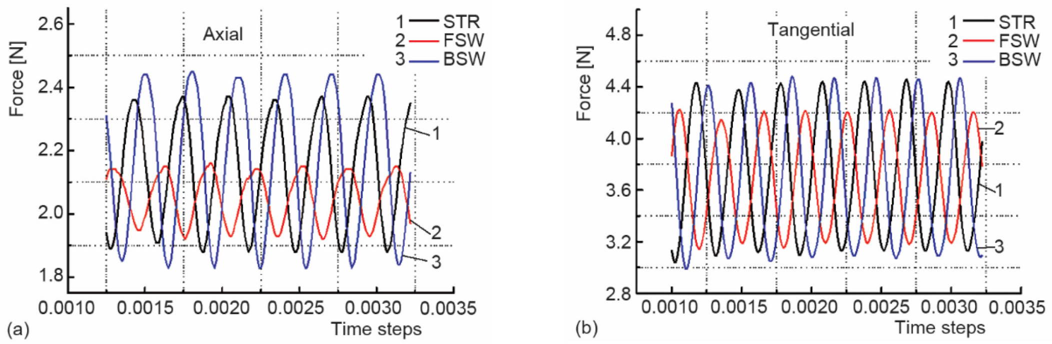

Figure 8. The axial and tangential excitation force of rotor at different time step

More results can be obtained from further analysis. That is, the first and the second order tangential excitation force factor are 0.175 and 0.0114, respectively, and the first and the second order axial excitation factor is 0.133 and 0.0099, respectively. The previous excitation factors are all in the normal range. The same analysis is applied to seven kinds of swept angle blades ranging from –15° to 15° with an interval of 5°. Table 1 shows the comparison of excitation factors obtained from blades with different swept angles.

Table 1. Excitation force factors of different cases

Blade type	Swept angle [°]	Tangential excitation force factor		Axial excitation force factor	
		First order	Second order	First order	Second order
Straight	0	0.175	0.0114	0.113	0.0099
FSW	5	0.159	0.0113	0.099	0.0080
	10	0.154	0.0085	0.070	0.0098
	15	0.139	0.0060	0.052	0.0074
BSW	5	0.180	0.0137	0.121	0.0119
	10	0.181	0.0170	0.128	0.0147
	15	0.187	0.0177	0.142	0.0142

Conclusions can be drawn from tab. 1 that, when the swept angle is small, the excitation factor of the FSW blade is decreased compared with STR, and the decreasing percentage is closely related to the swept angle. As for a BSW blade, the situation is the other way around. In addition, the variation in axial excitation factor is more obvious. The research shows that the FSW blade can effectively reduce the aerodynamic exciting force. On the one hand, the flow around the swept blade is more steady. The spanwise flow and trailing edge pressure of stator blade are under control. On the other hand, the gap between stator blade and rotor blade is increased, which is beneficial to the wake dissipation.

Conclusions

Due to the influence of geometric construction of swept blades, the streamline near the end wall shifts to the corner or mid-span in the span direction. For several models, it is observed that the unsteady pressure fluctuation of rotor happens because of the influence of upstream stator wakes. Moreover, compared with STR, the pressure fluctuation of FSW blade is decreased while the pressure fluctuation of BSW blade is increased. For seven kinds of swept blade models with different swept angles, the excitation force factors were obtained by spectral analysis, and the results of numerical simulation are reasonable because the previous excitation factors are all in the normal range. The excitation factor of the FSW blade is decreased compared with STR, and the decreasing percentage is closely related to the swept angle. As for a BSW blade, the situation is the other way around. In addition, the variation in axial excitation factor is more obvious. As a result, the vibration reduction performance of FSW blade is better.

Nomenclature

C_p – specific heat, [Jkg^{-1}K^{-1}]
E, F, G – convectional momentum flux, [kgs^{-2}m^{-1}]
E_v, F_v, G_v – viscosity momentum flux, [kgs^{-2}m^{-1}]
f – frequency, [Hz]
k – kinetic energy, [J]
p – pressure, [Pa]
T – temperature, [K]
t – time, [s]
U – velocity, [ms^{-1}]

Greek symbols

β – thermal expansion coefficient, [–]
ε – turbulent dissipation, [–]
λ – heat transfer coefficient, [Wm^{-2}K^{-1}]
μ – dynamic viscosity, [Pa·s]
ρ – density, [kgm^{-3}]

References

[1] Chaluvadi, V. S. P., *et al.*, Vortex Transport and Blade Interactions in High Pressure Turbines, *Enhanced Heat Transfer*, *126* (2004), 3, pp. 395-405
[2] Lampart, P., *et al.*, Investigations of Interaction of the Main Flow with Root and Tip Leakage Flows in an Axial Turbine Stage by Means of a Source/Sink Approach for a 3-D Navier-Stokes Solver, *Journal of Thermal Science, 10* (2001), 3, pp. 198-204
[3] Carolus, Th., Beiler, M., Skewed Blades in Low Pressure Fans – A Survey of Noise Reduction Mechanisms, *Proceedings,* 3rd AIAA/CEAS Aeroacoustics Conference, Atlanta, Geo., USA, 1997
[4] Corsini, A., *et al.*, Using Sweep to Extend the Stall-Free Operational Range in Axial Fan Rotors, *Proceedings,* the Institution of Mechanical Engineers, Part A: *Journal of Power and Energy*, *218* (2004), 3, pp. 129-139
[5] Clemen, C., *et al.*, Compressor Blades with Sweep and Dihedral: a Parameter Study, *Proceedings,* 5th European Conference on Turbomachinery Fluid Dynamics and Thermodynamics, Prague, Czech Republic, 2003
[6] Gallimore, S. J., *et al.*, The Use of Sweep and Dihedral in Multistage Axial Flow Compressor Blading – Part I, *Journal of Turbomachinery*, *124* (2002), 4, pp. 33-47
[7] Wennerstrom, A. J., Experimental Study of a High-Through Flow Transonic Axial Compressor Stage, *Journal of Engineering for gas turbines and Power*, *106* (1984), 3, pp. 552-560
[8] Kim, T. H., *et al.*, Numerical Investigation on the Effect of Blade Sweep on the Performance of Wells Turbine, *Renewable Energy*, *25* (2002), 2, pp. 235-248
[9] Sasaki, T., Breugelmans, F., Comparison of Sweep and Dihedral Effects on Compressor Cascade Performance, *Journal of Turbomachinery*, *120* (1998), 3, pp. 454-463
[10] Yakhot, V., Orszag, S. A., Renormalization-Group Analysis of Turbulence, *Physical Review Letters*, *57* (1986), 14, pp. 1722-1724

Paper submitted: February 7, 2016
Paper revised: March 20, 2016
Paper accepted: March 25, 2016